

## Short communication

Fabrication and properties of 3-D C<sub>f</sub>/ZrC–SiC composites  
via in-situ reactionQinggang Li<sup>a,c,\*</sup>, Shaoming Dong<sup>b,\*\*</sup>, Zhi Wang<sup>a</sup>, Guopu Shi<sup>a</sup>, Yan Ma<sup>a</sup>, Haijun Zhou<sup>b</sup>,  
Zhen Wang<sup>b</sup><sup>a</sup>School of Material Science and Engineering, University of Jinan, Jinan 250022, China<sup>b</sup>Structural Ceramics and Composites Engineering Research Center, Shanghai Institute of Ceramics, Chinese Academy of Sciences, Shanghai 200050, China<sup>c</sup>Shandong Provincial Key Laboratory of Preparation and Measurement of Building Materials, Jinan 250022, China

Received 17 February 2013; received in revised form 18 June 2013; accepted 4 July 2013

Available online 22 July 2013

## Abstract

Three-dimensional needled C<sub>f</sub>/ZrC–SiC composites were successfully fabricated via in-situ reaction using zirconium powders, silicon powders, and phenolic resin as raw materials. ZrC–SiC matrix is formed through the crystallization at relatively low temperature. The microstructures and mechanical properties of the composites were studied using X-ray diffraction, scanning electron microscopy, and three-point bending test. Their high-temperature oxidation resistance and anti-ablation properties were evaluated using a muffle furnace and the plasma wind tunnel test. The experimental results show that the composites have good mechanical and excellent ablative properties.

© 2013 Elsevier Ltd and Techna Group S.r.l. All rights reserved.

**Keywords:** A. Sintering; C. Mechanical properties; Ceramic–matrix composites; High-temperature properties; Microstructure evolution

## 1. Introduction

Carbon fiber-reinforced ultra-high temperature ceramic matrix (C<sub>f</sub>/UHTC) composites are emerging materials in improving the high-temperature performance of carbon fiber-reinforced silicon matrix (C<sub>f</sub>/SiC) composites in aerospace and related industries. C<sub>f</sub>/UHTC composites have received considerable attention due to their unique physicochemical and mechanical properties, such as increased durability, corrosion resistance, and good performance at elevated temperatures (> 2000 °C). In addition, they can take the place of C<sub>f</sub>/SiC composites, used in high-temperature structural elements for aerospace equipment, such as rocket nozzles, nosetip, aeronautic jet engines, and leading edges [1,2]. Therefore, C<sub>f</sub>/UHTC composites are one of the most promising materials in aerospace and military fields in the 21st century.

Ultrahigh-temperature ceramics (UHTCs) are introduced into the matrix of C<sub>f</sub>/SiC composites to fabricate C<sub>f</sub>/UHTC

composites. In our previous study, Wang et al. fabricated C<sub>f</sub>/UHTC composites using hot-pressing and polymer infiltration pyrolysis (PIP) [3], as well as mold-pressing and polymer infiltration and pyrolysis (PIP) [4]. Meanwhile, Li et al. reported the nature of ZrC precursor [5] and the fabrication and properties of C<sub>f</sub>/UHTC composites using ZrC precursor and polycarbosilane [6]. Recently, the fabrication and comparison of 3D C<sub>f</sub>/ZrC–SiC composites using ZrC particles/polycarbosilane and ZrC precursor/polycarbosilane was investigated [7]. Other techniques have also been utilized to fabricate C<sub>f</sub>/UHTC composites, including chemical vapor infiltration (CVI) combined with modified polymer infiltration pyrolysis (PIP) [8], and a soft-solution approach using an inorganic precursor [9], melt infiltration processing [10–13]. Although the above traditional preparation process have a series of advantages, some of these processes have obvious disadvantages, such as time-consuming, high-cost, and reduction of strength for the obtained component at elevated temperatures [14]. Thus, it is an eternal subject to fabricate advanced composite materials with high density and good performance and the preparation technology of composites with low-cost and high efficiency in composite materials

\*Corresponding author at: School of Material Science and Engineering, University of Jinan, Jinan 250022, China. Tel.: +86 18865906633.

\*\*Corresponding author.

E-mail addresses: [liqinggang66@gmail.com](mailto:liqinggang66@gmail.com) (Q. Li),  
[smdong@mail.sic.ac.cn](mailto:smdong@mail.sic.ac.cn) (S. Dong).

research field. On the other hand, composites fabricated by PIP process have low density, uneven structure and contain a lot of pores and micro-crack. It is known that a dense matrix is processed to protect the fibers and interfaces from the oxidation environment. Reaction sintering is one of the processes suitable for forming a dense matrix without firing shrinkage [15]. Reaction sintering is a simple and more cost effective method for the fabrication of ceramic matrix composites (CMCs) compared with CVI and PIP, in which the mixture of the raw materials is sintered directly. However, studies on  $C_f/ZrC-SiC$  composites manufactured through in-situ reaction sintering are limited.

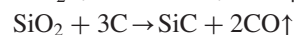
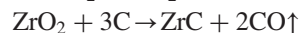
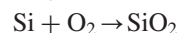
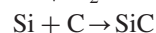
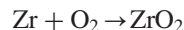
The present work aims to develop a new method for the fabrication of three-dimensional (3-D)  $C_f/ZrC-SiC$  composites based on our previous study. Our initial studies on the preparation of 3-D  $C_f/ZrC-SiC$  composites using zirconium powders, silicon powders, and thermosetting phenolic resin as raw materials are reported in this paper. The properties of the composites are also studied.

## 2. Experimental procedure

Carbon fibers (T300SC, Toray, Tokyo, Japan) with average diameter of 6  $\mu m$  were used for the current experiment. The 3-D fabrics were manufactured by Nanjing Fiberglass Research and Design Institute (Nanjing, China). The architecture had a fiber distribution of 8:2:1 in the x:y:z directions, respectively, and  $\sim 40\%$  fiber volume fraction. This preform is a PAN-derived needled felt. In addition, some 3-D fabrics were coated with PyC or PyC/SiC interphase via chemical vapor infiltration. Zirconium (Zr) powder ( $< 43 \mu m$ ,  $> 98$  wt% pure, High Purity Chemical, Saitama, Japan), silicon (Si) powder ( $< 10 \mu m$ , 99.9 wt% pure, High Purity Chemical, Saitama, Japan), and thermosetting phenolic resin (Shanghai Qinan Adhesive Material Factory, Shanghai, China) were first ball milled at an appropriate volume ratio to form a homogeneously dispersed slurry using ethyl alcohol as solvent. The contents of raw materials are as shown in Table 1. Thermosetting phenolic resin solution was applied as the carbon resource. The 3-D fabrics were then impregnated using the above-mentioned slurry. Thereafter, the samples were carried in a 120  $^{\circ}C$  rotating evaporator and pyrolyzed in a 900  $^{\circ}C$  vacuum carbon tube furnace with Argon gas for 30 min to obtain 3-D  $C_f/ZrC-SiC$  preforms. During the evaporation process, the ethanol evaporated completely and the phenolic resin already crosslinked. The obtained composites were further densified via four cycles of PIP process with the slurry mixture, and then pyrolyzed at 900  $^{\circ}C$  for 30 min at the same conditions. After pyrolysis, the samples were heated at 1500  $^{\circ}C$  in a high-temperature graphite resistance furnace at a rate of 10  $^{\circ}C/min$  with Argon gas for

60 min and then cooled the room temperature along with the furnace cooling, as shown in Fig. 1. During the process, some of the close pores were converted into open pores [3]. The in-situ reaction was accompanied by a 1500  $^{\circ}C$  heat-treatment process. During the in-situ reaction, Zr powders and Si powders were allowed to react with the carbon from the pyrolysis of thermosetting phenolic resin to form ZrC and SiC, respectively. The possible reactions during the pyrolysis and the heat-treatment process are as follows:

Phenolic resin  $\rightarrow C + \text{volatile} \uparrow$



The densities of the samples were measured using Archimedes' method. The samples were then cut into 4 mm  $\times$  5 mm  $\times$  60 mm specimens and polished for the three-point bending test in an Instron-5566 testing machine with a cross-head speed of 0.5 mm/min and a span of 48 mm. Both the polished cross sections and the fracture surface of the composites were studied using an Electron Probe Micro-analyzer (EPMA, JXA-800, Jeol, Tokyo, Japan) equipped with an energy-dispersive spectrum (EDS, INCA, Oxford, Tokyo, Japan).

The anti-ablation test was performed in a plasma wind tunnel environment [the National Military Standard of the People's Republic of China (FL 0183, GJB 323A-96)], with approximately  $25,120 \pm 2512$  kW/m<sup>2</sup> heat flux and 2400 K flame temperature. Nitrogen pressure was 0.5 MPa, whereas the gas flow rate was 13,596 L/h. The arc voltage and arc current were  $185 \pm 5$  V and  $550 \pm 10$  A, respectively, whereas the pressure of cool water and heater power were 1.5 MPa and approximately 100 Kw, respectively. The nozzle diameter and electrode distance were 8 mm and 3.3–4.0 mm, respectively. During the test, the specimen with a size of 80 mm  $\times$  80 mm  $\times$  10 mm was vertically exposed to the flame for 600 s when the surface temperature of the composite reached 2400 K. The distance between the nozzle tip and the surface of the specimen was  $10 \pm 0.2$  mm and the flame ablation angle was 90 $^{\circ}$ . The compositions of the composites before and after ablation were characterized through X-ray diffraction (XRD)

Table 1  
The content of raw materials.

Raw materials	Zr powder	Si powder	Phenolic resin
Content (wt%)	60	8	32

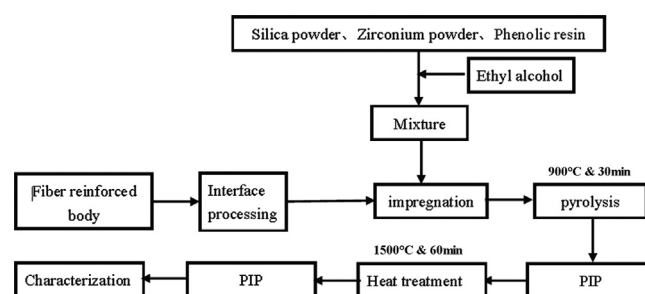


Fig. 1. Experimental procedure for preparation of 3-D  $C_f/ZrC-SiC$  composites.

with Cu  $K_\alpha$  radiation. The surface temperature of the sample was monitored using an optical pyrometer. The microstructures of the composites after ablation were studied by VHX-600E Series Digital Microscope (Osaka, Japan).

### 3. Results and discussions

The physical and mechanical properties of the 3-D  $C_f/ZrC-SiC$  composites with different interphases were investigated. The results show that the samples without interphases have higher densities ( $2.48 \text{ g/cm}^3$ ), and open porosity of 8%. However, the composites with PyC/SiC and PyC interphases

between the fiber and matrix exhibits lower densities, and higher open porosities than those without interphases ( $2.16$  and  $2.10 \text{ g/cm}^3$  for the composites with PyC/SiC and PyC interphases, respectively, and 15% and 16% open porosities for the composites with PyC/SiC and PyC interphases, respectively). The existence of interphases (PyC or PyC/SiC) prevents Zr powders and Si powders from going through the wrapped bundles in the impregnation process. Hence, composites without interphases have higher densities, and lower open porosities. Compared with our previous studies [5–7], the present process is simple and cost effective because it can be in less cycle to acquire higher density.

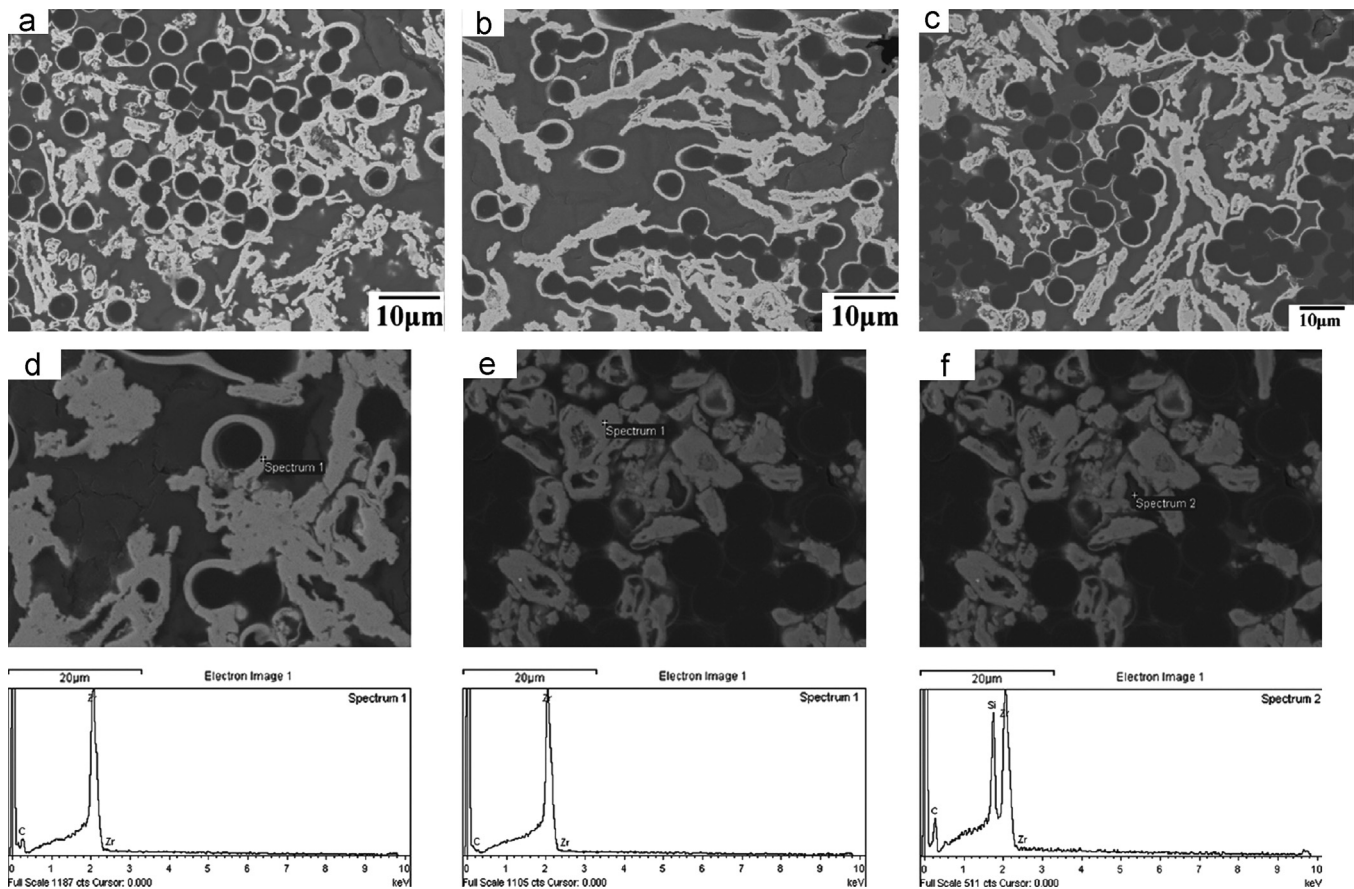


Fig. 2. Back-scattered electron images for the polished cross sections and electron probe microanalyzer micrographs and energy-dispersive spectrum analysis of 3-D  $C_f/ZrC-SiC$  composites: (a) none; (b) PyC interphase; (c) PyC/SiC interphase; (d) a ZrC coating; and (e) and (f) a core-shell encapsulation structure.

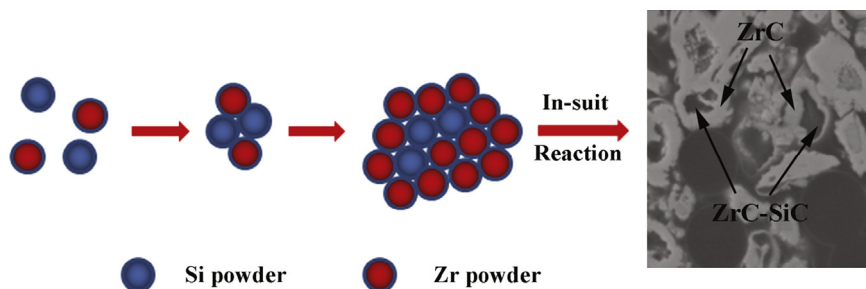


Fig. 3. The forming process of core-shell encapsulation structure.



The micrographs of the polished cross sections of composites with different interphases (Fig. 2) show that the UHTCs are almost evenly distributed in the interbundle matrix and the interbundle matrix is almost fully dense. Based on Fig. 2(a)–(f), a coating is formed on the surface of the fibers, and the matrices exhibit a core–shell encapsulation structure. Fig. 2(d) shows that the coating on the surface of the fibers is ZrC. Moreover, Fig. 2(e) and (f) shows that the shell of the core–shell encapsulation structure is ZrC, and the core is a mixture of ZrC and SiC. The forming process of the special structure is shown in Fig. 3. During the PIP process, Zr powders and Si powders stick together under the action of the thermosetting phenolic resin. Because Zr powders have a large proportion, redundant Zr powders are wrapped in the outer layer. In the in-situ reaction process, the C atoms from the thermosetting phenolic resin diffuse into the Zr and Si sites and form the ZrC and SiC in-situ, respectively. This observation means that 3-D  $C_f/ZrC-SiC$  composites can be produced through this in-situ reaction.

The typical bending stress–displacement curves of all composites with different interphases are shown in Fig. 4. From Fig. 4, all composites show sudden failure from the point of ultimate strength except the composite having interphase, such as  $C_f-PyC/SiC$ . In that case, interphase is playing a key role in the failure mechanism. Based on Fig. 4, the composites with interphases have bending stress of approximately  $290 \pm 14$  MPa. However, the composite without interphase has a bending stress of  $257 \pm 21$  MPa. Fig. 2(a) shows that a ZrC coating is formed on the surface of fibers. To some extent, the ZrC coating plays the

role of PyC or PyC/SiC interphase, which can be explained by the bonding strength between the fibers and the matrix. The ZrC interphases result in a weak bonding between the fibers and matrix when the ZrC coating as interphase is formed in the in-situ reaction process. This condition facilitates crack deflection and fiber pull-out, which are beneficial for the improvement of fracture toughness. Thus, the in-situ reaction to fabricate 3-D  $C_f/ZrC-SiC$  composites weakens the effect of interphases on the composites. This method can shorten the fabrication cycle and has an important impact on the fabrication of the 3-D  $C_f/ZrC-SiC$  composites. In addition, this method can enable the composites without interphase to have enough strength to meet the operation requirements.

The morphologies of the fracture surfaces are shown in Fig. 5. All composites exhibit fiber pull-outs during the fracture process for all the composites. However, the pulled-out fibers are short when no interphase is deposited. In contrast, the pulled-out fibers are longer with PyC/SiC or PyC interphases. This phenomenon can also be explained by the bonding strength between the fibers and the matrix, which also shows that the matrix is almost fully dense in the interbundle. During the reaction, normally formation of ZrC takes place first, than formations of SiC takes place due to their difference in free energies. In that case, ZrC forms first around the fibers, at the same time, during high temperature treatment ZrC alone deteriorates the properties of fibers by formations of ZrC on the carbon surface. In such case, interphase can inhibit the formation of ZrC at the surface of carbon.

The high-temperature property of the  $C_f/UHTC$  composite is important: hence, the 3-D  $C_f/ZrC-SiC$  composite with PyC/SiC interphases was evaluated via a plasma wind tunnel test. Fig. 6 shows the morphologies of the 3-D  $C_f/ZrC-SiC$  composite before (Fig. 6a), and after (Fig. 6c) the plasma wind tunnel test. Fig. 6(d) and (e) shows the XRD patterns of the composite before and after testing. The comparison between Fig. 6a and c shows that the shape and surface of the composite remain intact, and that the composite is almost without ablation. In addition, Fig. 6(c) shows that three regions are formed on the surface, namely, (A)—the ablation center region, (B)—the ablation transition region, and (C)—the unablation region. The diffraction peaks in Fig. 6d shows that the main phases existing in the composite are ZrC and SiC. Moreover, the results validate the EDS analysis of the polished cross-sectional surface. Fig. 6e shows that a glass layer of  $SiO_2$  and  $ZrO_2$  is formed when the composite was tested in the plasma wind tunnel atmosphere, which mainly contributes to the excellent

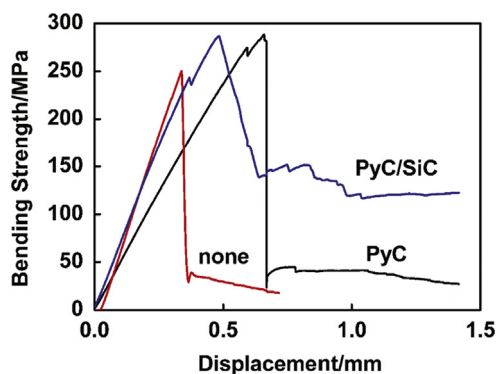


Fig. 4. Bending stress/displacement curves of 3-D  $C_f/ZrC-SiC$  composites with different interphases.

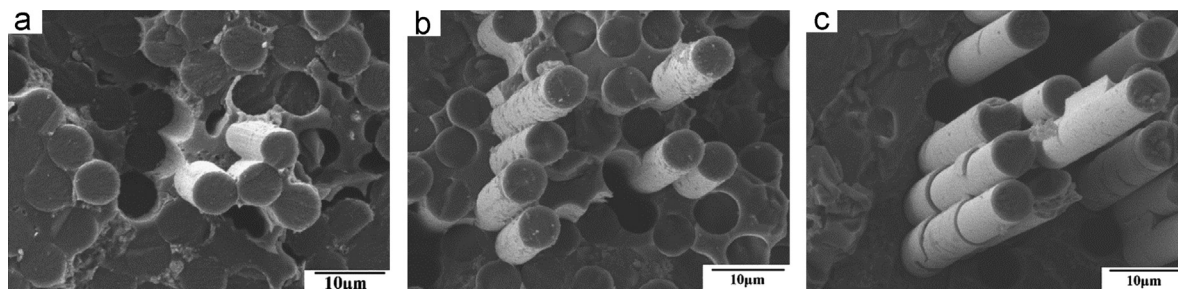


Fig. 5. SEM micrographs of the fracture surfaces of the 3-D  $C_f/ZrC-SiC$  composites with different fiber fractions: (a) none; (b) PyC interphase; and (c) PyC/SiC interphase.

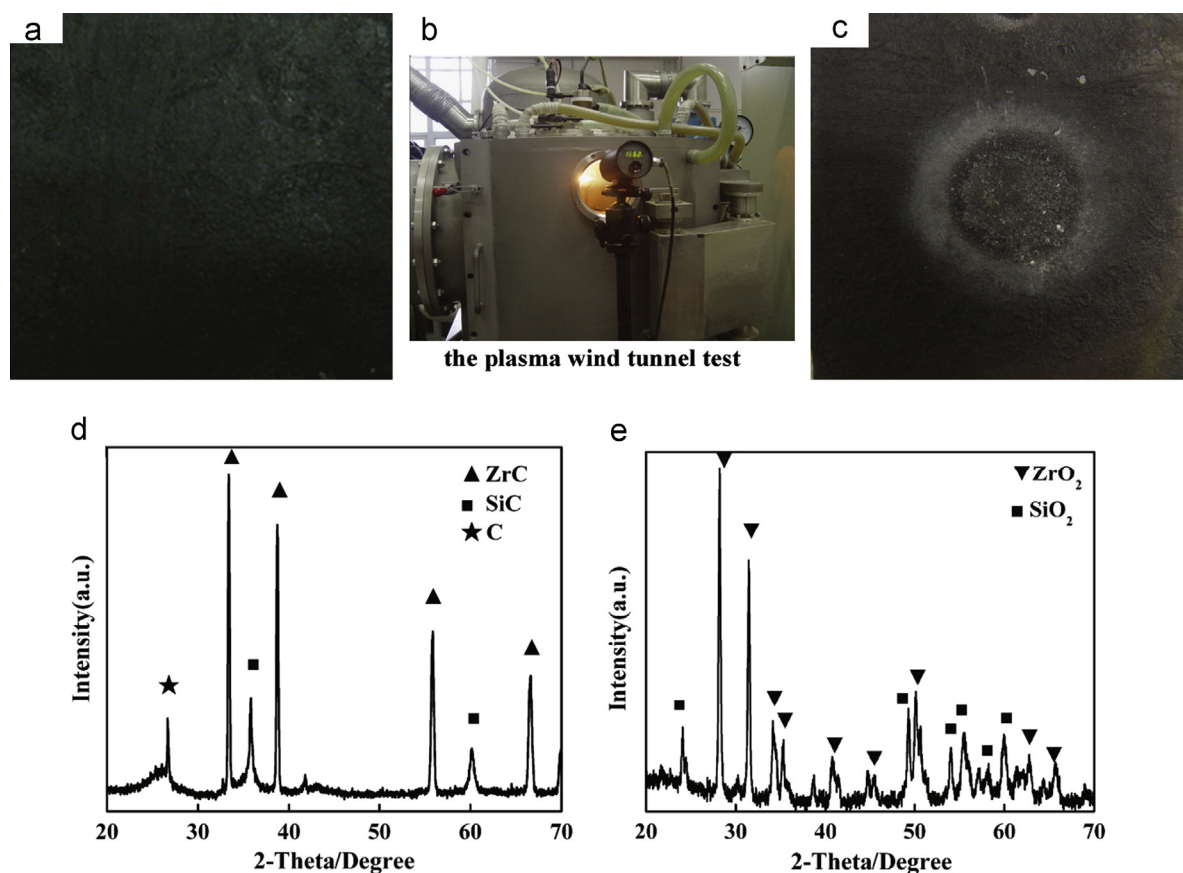


Fig. 6. The plasma wind tunnel test of 3-D  $C_f/ZrC-SiC$  composite: (a) before ablation; (b) in the middle of ablation; (c) after ablation; (d) XRD pattern of the composite before ablation; and (e) XRD pattern of the composite after ablation.

anti-ablation properties. The mass loss rate and linear recession rate of the composite during the plasma wind tunnel test are 0.001 g/s and  $-0.0009$  mm/s, respectively. Therefore, compared with my previous studies [5–7] the 3-D  $C_f/ZrC-SiC$  composites have excellent high-temperature properties.

#### 4. Conclusions

The 3-D  $C_f/ZrC-SiC$  composites were fabricated via in-situ reaction using zirconium powders, silicon powders, and phenolic resin as raw materials. All composites exhibit typical non-brittle fracture behavior. A ZrC coating is formed on the surface of the fibers, and the matrices exhibit a core-shell encapsulation structure. The in-situ reaction to fabricate the 3-D  $C_f/ZrC-SiC$  composites weakens the effect of interphases on the composites, which can shorten the fabrication cycle and has an important impact on the fabrication of the 3-D  $C_f/ZrC-SiC$  composites. In addition, this method can enable the composites without interphase to have enough strength to meet the operation requirements. Based on the findings from this research, the composites have excellent high-temperature properties.

#### Acknowledgments

Authors appreciate the financial support of the National Natural Science Foundation of China under the Grant nos.

51172256 and 51142010, and Innovation Program of Shanghai Institute of Ceramics Chinese Academy of Sciences under Grant no. Y12ZC6160G and the Doctoral Fund of University of Jinan (XBS1310). Authors also appreciate the financial supported by Program for Scientific research innovation team in Colleges and universities of Shandong Province. Authors also thank Professor Xiaolei Wu and Professor Heji Huang from Institute of Mechanics Chinese Academy of Sciences for the plasma wind tunnel test.

#### References

- [1] S. Schmidt, S. Beyer, H. Knabe, H. Immich, R. Meistring, A. Gessler, Advanced ceramic matrix composite materials for current and future propulsion technology applications, *Acta Astronautica* 55 (2004) 409–420.
- [2] W. Krenkel, B. Heidenreich, R. Renz, C/C–SiC composites for advanced friction systems, *Advanced Engineering Materials* 4 (2002) 427–436.
- [3] Z. Wang, S.M. Dong, X.Y. Zhang, H.J. Zhou, D.X. Wu, Q. Zhou, D.L. Jiang, Fabrication and properties of  $C_f/SiC-ZrC$  composites, *Journal of the American Ceramic Society* 91 (10) (2008) 3434–3436.
- [4] Z. Wang, S.M. Dong, Y.S. Ding, X.Y. Zhang, H.J. Zhou, J.S. Yang, B. Lu, Mechanical properties and microstructures of  $C_f/SiC-ZrC$  composites using T700SC carbon fibers as reinforcements, *Ceramics International* 37 (2011) 695–700.
- [5] Q.G. Li, H.J. Zhou, S.M. Dong, Z. Wang, P. He, J.S. Yang, B. Wu, J.B. Hu, Fabrication of a ZrC–SiC matrix for ceramic matrix composites and its properties, *Ceramics International* 38 (2012) 4379–4384.

- [6] Q.G. Li, S.M. Dong, Z. Wang, P. He, H.J. Zhou, J.S. Yang, B. Wu, J.B. Hu, Fabrication and properties of 3-D C<sub>f</sub>/SiC–ZrC composites, using ZrC precursor and polycarbosilane, *Journal of the American Ceramic Society* 95 (4) (2012) 1216–1219.
- [7] Q.G. Li, H.J. Zhou, S.M. Dong, Z. Wang, J.S. Yang, B. Wu, J.B. Hu, Fabrication and comparison of 3D C<sub>f</sub>/ZrC–SiC composites using ZrC particles/polycarbosilane and ZrC precursor/polycarbosilane, *Ceramics International* 38 (6) (2012) 5271–5275.
- [8] H.B. Li, L.T. Zhang, L.F. Cheng, Y.G. Wang, Fabrication of 2D C/ZrC–SiC composite and its structural evolution under high-temperature treatment up to 1800, *Ceramics International* 35 (2009) 2831–2836.
- [9] N. Padmavathi, S. Kumari, V.V.B. Prasad, J. Subrahmanyam, K.K. Ray, Processing of carbon-fiber reinforced (SiC+ZrC) mini-composites by soft-solution approach and characterization, *Ceramics International* 35 (2009) 3447–3454.
- [10] Y.G. Wang, X.J. Zhu, L.T. Zhang, L.F. Cheng, Reaction kinetics and ablation properties of C/C–ZrC composites fabricated by reactive melt infiltration, *Ceramics International* 37 (2011) 1277–1283.
- [11] Y.G. Tong, S.X. Bai, K. Chen, C/C–ZrC composite prepared by chemical vapor infiltration combined with alloyed reactive melt infiltration, *Ceramics International* 38 (2012) 5723–5730.
- [12] H.L. Pi, S.W. Fan, Y.G. Wang, C/SiC–ZrB<sub>2</sub>–ZrC composites fabricated by reactive melt infiltration with ZrSi<sub>2</sub> alloy, *Ceramics International* 38 (2012) 6541–6548.
- [13] Y.L. Zhu, S. Wang, H.M. Chen, W. Li, J.M. Jiang, Z.H. Chen, Microstructure and mechanical properties of C<sub>f</sub>/ZrC composites fabricated by reactive melt infiltration at relatively low temperature, *Ceramics International*, <http://www.dx.doi.org/10.1016/j.ceramint.2013.05.004>.
- [14] S.R. Zbigniew, A process for C<sub>f</sub>/SiC composites using liquid polymer infiltration, *Journal of the American Ceramic Society* 84 (10) (2001) 2235–2239.
- [15] G.S. Corman, M.K. Brun, K.L. Lthra, ASME Paper 99-GT-234, in *International Gas Turbine and Aeroengine Congress and Exposition*, Indianapolis, Indiana, USA, June 7–10, 1999.